Indian Journal of Chemistry
Vol. 62, November 2023, pp. 1162-1170
DOI: 10.56042/ijc.v62i11.2610

Synthesis of novel anticancer coumarin-triazole-chalcone hybrids as potential AKT inhibitors

E Mallikarjun[b], D Suneesha[b], A Niranjana Kumar[a], Akanksha Singh[c], Hashnu Dutta[d], J Kotesh Kumar*[a], K V N Satya Srinivas*[a], Abha Meena[c], B Venkatesh[a], Nishant Jain[d], Sravanthi[b] & T Radhika[b]

[a] Phytochemistry Division, CSIR-Central Institute of Medicinal and Aromatic Plants, Research Centre, Boduppal, Hyderabad 500 092, India

[b] Department of Pharmaceutical Chemistry, G. Pulla Reddy College of Pharmacy, Hyderabad 500 028, India

[c] Bioprospection and Product Development Division, CSIR-Central Institute of Medicinal and Aromatic Plants, Lucknow 226 015, Uttar Pradesh, India

[d] Department of Applied Biology, CSIR-Indian Institute of Chemical Technology, Hyderabad 500 007, Telangana State, India

E-mail: koteshkumarj@cimap.res.in, kvn.satyasrinivas@cimap.res.in

Received 13 June 2023; accepted (revised) 19 October 2023

This research article presents the synthesis of a novel series of hybrid analogues of Coumarin-Triazole-Chalcone, which are potential bioactives with a novel mode of action for anticancer therapy. The compounds have been synthesized *via* aldol condensation and 1,3-dipolar cycloaddition, resulting in the generation of hybrid heterocyclic systems that combine two or more pharmacophores. The synthesized compounds have then been screened for anticancer activity against various human cancer cell lines, including A549 (lung cancer), HeLa (Cervix carcinoma), PANC1 (pancreatic cancer), HT1080 (Fibrosarcoma) and HEK293 (Human embryonic kidney cells), *in vitro*. One of the compounds, *para*-nitrile chalcone **9a**, demonstrates significant IC_{50} values in the range of 3.1 to 7.02 µg/mL when compared to the others. All the compounds **9a**-**d** have shown higher IC_{50} values towards HEK-293 cells indicating their non-toxic nature towards normal cells. Furthermore, *in silico* approaches have been employed to assess the efficacy of compounds that are active in the MTT assay against molecular targets. The authors conducted docking studies of the proteins PI3K and AKT, which are common target biomarkers in Pancreatic cancer, Lung cancer, Cervical cancer, and Fibrosarcoma, with compound **9a** and some known inhibitors. The results show that compound **9a** has a good binding affinity with AKT (–10.6) and PI3K (–10.3). However, it is found to be more specific for AKT as its binding site amino acid interactions are similar to those of known AKT inhibitors. These findings provide evidence that hybrid heterocyclic systems may be useful for developing potential bioactives with a novel mode of action for anticancer therapy.

Keywords: Coumarins, 1,2,3-Triazole, Chalcones, Anticancer Activity, Molecular docking

Pursuit of development of a potential lead molecule for a specific disease has lead to the generation of hybrid pharmacophore concept in which two or more different heterocyclic moieties having different bioactivity profiles are combined to result in a single molecules having complementary drug actions and unique mode of actions[1]. To develop such hybrid systems with structural diversity, known pharmacophores such as coumarins, 1,2,3-triazoles and chalcones were selected. Coumarins are important class of oxygen containing heterocyclic compounds also known as 1,2-benzopyrone, 2*H*-chromen-2-one or 2-oxo-1,2-benzopyran[2]. These naturally occurring molecules are widely expressed by plants and can be synthesised in the laboratory[3]. Both natural and synthetic coumarins are endowed with a great therapeutic potential due to the wide spectrum of biological properties including anticancer, antimicrobial, antiviral, anti-inflammatory, neuroprotective, and antioxidant activities.

During the recent past, 1,2,3-triazoles have received attention as a potential pharmacophore such as anticancer, and antituberculosis, antivirus, *etc*.[4,5] Derivatization of plant bioactives with substituted 1,2,3-triazoles such as podophyllotoxin-1,2,3-triazoles (**I**)[6], Forskolin-1,2,3-triazoles (**II**)[7], Andrographolide-1,2,3-triazoles (**III**)[8], combretastatin A-4 triazoles[9], artemisinin 1,2,3-triazoles[10], dehydroabietic acid 1,2,3-triazoles[11] have shown different predominant biological activities.

On the other hand, Chalcones constitute an important class of natural products belonging to the flavonoid family, which display large number of

biological activities like anti-inflammatory[12], antibacterial[13], antioxidant[14], antimalarial[15] and anticancer[16]. They are also effective in *in vivo* as cell proliferating inhibitors, anti-tumor promoting and chemo preventing agents. A number of clinically useful anticancer drugs have genotoxic effects due to interaction with the amino groups of nucleic acids but chalcones were found to be devoid of this important side effect[17]. Our earlier research on pharmacophore combinations such as Eugenol-1,2,3-triazoles (**IV**)[18], chalcone-1,2,3-triazoles (**V**)[19], *etc*., resulted in production of anticancer and hypolipidemic active analogues (Fig. 1).

Influenced by the above, and as a continuing activity, we have developed few novel adducts of Coumarin-1,2,3-triazole-chalcones that have shown potent, selective and less toxic bioactive properties. The novel Coumarin-1,2,3-triazole-chalcone were synthesized by employing Cu(I)-catalysed Huisgen [3+2] cycloaddition (click chemistry). The resulting analogues were tested for their anticancer activity potentials in *in vitro* mode against selected human cancer cell lines such as A549 (lung cancer), HeLa (Cervix carcinoma), PANC1 (pancreatic cancer) and HT1080 (Fibrosarcoma). *In silico* docking and ADMET studies were developed against most common target biomarkers PI3K and AKT and the binding efficacy of the most potent synthesized analogue was compared with some of the known inhibitors.

Experimental Section

Chemicals

All chemicals and reagents were purchased from Aldrich (India), AVRA Chemicals Pvt. Ltd. (India) and were used without further purification. TLC Silica gel 60 F_{254} (Merck, Germany) was used for TLC. Visualization of the developed TLC was performed by UV light or charring in 5% H_2SO_4 in MeOH.

Structural Characterization techniques

IR spectra were recorded on a Bruker Optics (Tensor 27 model, Germany) FT-IR spectrophotometer (using KBr pellets) and reported in wave number (cm^{-1}). ^{1}H NMR (300/400 MHz) spectra were measured in $CDCl_3$ and DMSO at RT on a Bruker Avance-III 300/400 MHz (Switzerland) instruments. The Chemical shifts are reported as δ parts per million (ppm) in $CDCl_3$ and DMSO using tetramethylsilane as an internal standard. Data are reported as follows: chemical shift, multiplicity (s: singlet, d: doublet, t: triplet, dd: doublet of doublet, q: quartet, br: broad, m: multiplet), coupling constants (*J* in Hz) and integration.

General procedure and spectral data of synthesized compounds

Synthesis of 7-hydroxy-4-ethylchloro coumarin, 3

To an equivalent mixture of resorcinol (**1**, 1.1 g, 10.0 mmol) and ethyl-4-chloroacetoacetate (2, 1.3 g, 10.0 mmol) was added TsOH (*para*-toluene sulfonic acid monohydrate) (0.09 g, 0.5 mmol) in a mortar and ground well with a pestle at RT. The mixture was heated at 60°C for 10 min under atmosphere. After cooling, water was added to the reaction mixture and the obtained crude product was subjected to Silica-gel

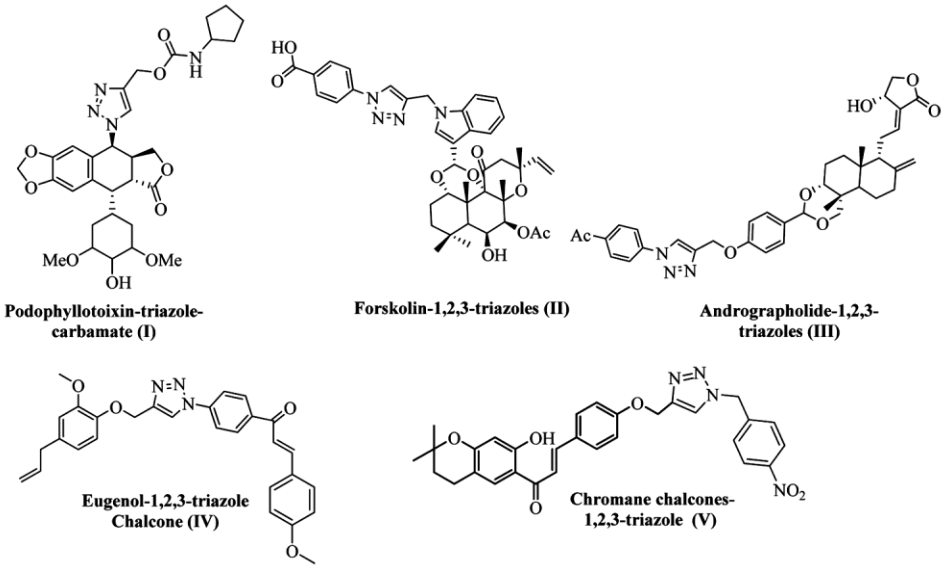

Fig. 1 — Structures of some biologically active derivatives

(100-200) mesh column chromatography using 10% ethyl acetate in *n*-hexane as mobile phase to give pure **3**.

Propargylation of 7-hydroxy-4-ethylchloro coumarin, 3

To a solution of **3** (1 equi., each) and potassium carbonate (1.5 equ.) in DMF (20 mL), propargyl bromide (0.7 mL g, 6.5 mmol) was added drop wise and the resulting mixture was allowed to stir for four hours at RT. After completion of reaction, as monitored by TLC, the reaction mixture was poured into water (500 mL each) drop wise and the resulting precipitate was filtered. The obtained solid portion was repeatedly washed with water to obtain the desired propargylated compound 4-(chloromethyl)-7-(prop-2-yn-1-yloxy)-2*H*-chromen-2-one **4** inpure from.

Synthetic procedures for 4-azidoacetophenone, 6

4-Aminoaetophenone **5** was dissolved in H_2O:HCl (1:1) and stirred at 0-5°C for 30 min. The aqueous $NaNO_2$ was added drop wise to diazotize amine hydrochloride. After stirring at 0-5°C, the solution was treated with aqueous NaN_3 and further stirred for 1 h. Finally, the reaction mixture was extracted with 5% ethyl acetate in hexane, dried over anhyd. Na_2SO_4 and concentrated *in vacuo* to afford 4-azidoacetophenone **6** in quantitative yield.

Procedure for the synthesis of azido-chalcones, 8a-d

Azido derivative **6** (1.0 eq.) and different substituted aromatic aldehydes (**7a-d**, 1.5 eq.) are dissolved in ethanol. To this reaction mixture, KOH (1.5 eq.) was added and stirred at 35-40°C for two hours. Then reaction mixture was diluted with ice cold distilled water (500 mL) and stirred for 30 min, resulted solid filtered and the filtrate was washed with water then with methanol, and recrystallized form petroleum ether to get yellow needles **8a-e** in pure from.

Synthesis of chalcones triazole derivatives, 9a-d

Intermediate 4-(chloromethyl)-7-(prop-2-yn-1-yloxy)-2H-chromen-2-one **4b** (1.0 equv. each) was dissolved separately in dry THF (20 mL) and catalytic amount of copper iodide was added. To this, azido-chalcones (**8a-d**, 1.0 equiv), in dry THF, were added slowly while stirring at RT under nitrogen atmosphere after overnight period the solvent was removed under reduced pressure and the residue was diluted with distilled water and extracted thrice with ethyl acetate. The combined organic layers were dried over anhyd. Na_2SO_4 and concentrated to get the product. The crude product was purified by column chromatography with ethyl acetate in hexane to get desired products coumarin-ethylchloro-1,2,3-triazole chalcones **9a-d**.

(E)-4-(3-(4-(4-(((4-(chloromethyl)-2-oxo-2*H*-chromen-7-yl)oxy)methyl)-1*H*-1,2,3-triazol-1-yl)phenyl)-3-oxoprop-1-en-1-yl)benzonitrile, 9a: Yellow solid. Yield 91%. IR (KBr): 2958, 2227, 1718, 1664, 1600, 1502, 1440, 1330, 1261, 1215, 1099, 1170, 1022, 819 cm^{-1}; ^1H NMR (DMSO-d_6, 400 MHz): δ 8.36 (d, *J* = 8.8 Hz, 1H), 8.23 (dd, *J* = 13.7, 8.8 Hz, 1H), 7.85 (m, 4H), 7.81 (d, *J* = 8.7 Hz, 4H), 7.78 (d, *J* = 8.4 Hz, 1H), 7.72 (m, 3H), 7.70 (m, 1H), 5.60 (d, *J* = 2.7 Hz, 2H), 4.05 (m, 2H); ESI-MS: negative ion mode: *m*/*z* Obsd: 539.5 [M+H_2O-1], Calcd for $C_{29}H_{19}ClN_4O_4$: 522.95.

(E)-7-((1-(4-(3-(4-(benzyloxy)phenyl)acryloyl)phenyl)-1*H*-1,2,3-triazol-4-yl)methoxy)-4-(chloromethyl)-2*H*-chromen-2-one, 9b: Yellow solid. Yield 90%, IR (KBr): 2918, 1720, 1600, 1508, 1380, 1263, 1170, 821 cm^{-1}; ^1H NMR (DMSO-d_6, 400 MHz): δ 8.37 (d, *J* = 8.4 Hz, 1H), 8.15 (dd, *J* = 20.3, 11.3 Hz, 1H), 8.10 (m, 2H), 7.95 (d, *J* = 14.9 Hz, 2H), 7.76 (d, *J* = 14.7 Hz, 2H), 7.27 (m, 3H), 7.22 (m, 4 H), 5.86 (s, 2H), 5.31 (d, *J* = 19.3 Hz, 2H), 4.86 (s, 2H).

(E)-3-(3-(4-(4-(((4-(chloromethyl)-2-oxo-2*H*-chromen-7-yl)oxy)methyl)-1*H*-1,2,3-triazol-1-yl)phenyl)-3-oxoprop-1-en-1-yl)benzonitrile, 9c: Yellow solid. Yield 92%, IR (KBr): 3262, 2820, 2278, 1712, 1600, 1503, 1304, 1274, 1147, 1022, 817 cm^{-1}; ^1H NMR (DMSO-d_6, 400 MHz): δ 8.55 (s, 1H), 8.45 (t, *J* = 9.2 Hz, 1H), 8.23 (m, 5H), 7.92 (d, *J* = 7.3 Hz, 2H), 7.85 (m, 2H), 7.69 (t, *J* = 7.8 Hz, 4H), 5.84 (s, 2H), 4.86 (dd, *J* = 27.8, 16.0 Hz, 2H); ESI-MS: negative ion mode: *m*/*z* Obsd: 539.5 $[M+H_2O-1]^-$, Calcd for $C_{29}H_{19}ClN_4O_4$: 522.95.

(E)-7-((1-(4-(3-(4-bromophenyl)acryloyl)phenyl)-1*H*-1,2,3-triazol-4-yl)methoxy)-4-(chloromethyl)-2*H*-chromen-2-one, 9d: Yellow solid. Yield 94%, IR (KBr): 2927, 2376, 1780, 1610, 1493, 1371, 1259, 1211, 1159, 1026, 842 cm^{-1}; ^1H NMR (DMSO-d_6, 400 MHz): δ 9.12 (d, *J* = 14.5 Hz, 1H), 8.77 (s, 2H), 8.56 – 8.37 (m, 3H), 8.27 – 8.06 (m, 3H), 7.97 – 7.65 (m, 2H), 7.09 (dd, *J* = 8.7, 2.6 Hz, 2H), 6.24 (d, *J* =

1.1 Hz, 1H), 5.41 (s, 2H), 4.81 (s, 2H); ESI-MS: positive ion mode: *m*/*z* Obsd: 594.1 $[M+H_2O]^+$, Calcd for $C_{28}H_{19}BrClN_3O_4$: 576.83.

In silico molecular docking

The virtual screening study includes the preparation of ligands and proteins, molecular interaction studies, drug-likeness and ADMET.

Preparation of Ligand

The chemical structure of synthesised compounds was drawn using ACD/ChemSketch (Freeware) software. The constructed structure was saved in MDL Molfile format. The 3D structures of inhibitors were downloaded from the PubChem database in SDF file format. In order to conduct further studies, MDL Molfile and SDF file of compounds and inhibitors were converted into the PDB file using PyMOL Molecular Graphics System, Version 1.5.0.4 Schrodinger, LLC, USA tool[20].

Preparation of Protein

The 3D crystal structures of receptor protein succinatedehydrogenase (SDH, 6VAX), Phosphoinositide-3-kinase (PI3K, 8EXL) and Protein kinase B (AKT, 1O6L) were retrieved from the RCSB Protein data bank. The PyMOL Molecular Graphics System, Version 1.5.0.4 Schrodinger, LLC, USA program was used to prepare the downloaded 3D structures of the target protein for *in silico* studies[21]. Before performing docking experiment, water molecules, undesirable heteroatoms, solvents, protonating residues, alternate conformations, and ligands were removed, and polar hydrogen atoms were added to receptor protein. The filtered crystallographic structures were afterwards saved in a PDB file for further studies[22].

Molecular Interactions

AutoDock (V. 4.0) was used in the PyRx interface for molecular docking studies. Each ligand was manually uploaded onto the program. One ligand at a time, subjected to energy minimisation, and then automatically converted into PDBQT format. The virtual screening process also involves setting up the grid box for desired docking site. During the docking, the protein was set as rigid and the ligand as flexible. Grid configuration file generated by PyRx Auto Grid engine[23]. The minimum binding energy with RMSD (root-mean-quarter deviation) values less than 1.0 were regarded as ideal for the ligand-protein interactions. The protein and ligand complexes with the lowest binding affinities were then visualised in BIOVIA Discovery Studio 2021 to analyse the binding pocket and poses of the ligand interactions. Further to confirm the stability of the protein-ligand complex, molecular dynamics simulations were performed with the help of a web tool, *i.e*. CABS-flex. The molecular dynamic simulations can assess ligand-induced alterations in protein structure[24]. The CABS-flex demonstrated the root mean square fluctuations experienced by the protein-ligand complex and protein alone.

Drug Likeness and ADMET

To predict pharmacokinetics properties, the compound with the highest binding affinity was chosen to evaluate drug-likeness and ADMET properties using online web tool Molinspiration, ADMETlab2.0, and pkCSM. To evaluate the oral administration of molecules, Lipinski's rule of five takes some factors into account, such as the molecular weight (MW), the log of the n-octanol/water partition coefficient (LogP), the hydrogen bond acceptors (nHBAs), and the hydrogen bond donors (nHBDs). In addition to -likeness, other crucial pharmacological parameters such as Caco2 permeability, intestinal absorption, cytochrome P450, AMES toxicity, skin sensitisation, BBB and CNS permeability were determined[25].

Results and Discussion

Chemistry

Synthesis of Coumarin Triazole chalcones

In the first step, Resorcinol **1** was reacted with ethyl 4-chloroacetoacetate **2** in the presence of *para*-toluene sulfonic acid monohydrate to give 7-Hydroxy-4-ethylchloro coumarin **3**. Later, propargylation was carried out and yielded propargylated derivative **4.** Now 4-acetophenone azide **6** was coupled with different aromatic aldehydes **7a-d** *via* aldol condensation to give respective azide chalcones **8a-d**. Then, propargylated derivative **4** coupled with different substituted azides by employing facile 1,3 dipolar cycloaddition to get distinct derivatives of Coumarin 1,2,3-triazol-chalcones (**9a-d**, Scheme 1).

^{1}H NMR of all the 4-methylcoumarin triazole chalcone derivatives **9a-d** has shown a characteristic singlet for triazole proton in the range δ 8.36-8.55 ppm. All the aromatic protons displayed signals in the range of δ 6.5-8.2ppm. The characteristic methyl proton was shown at δ 2.5 ppm. In IR spectra, the sharp bands at 1718 cm^{-1} and 2958 cm^{-1} indicated the presence of a keto group and a cyano moiety in **9a**.

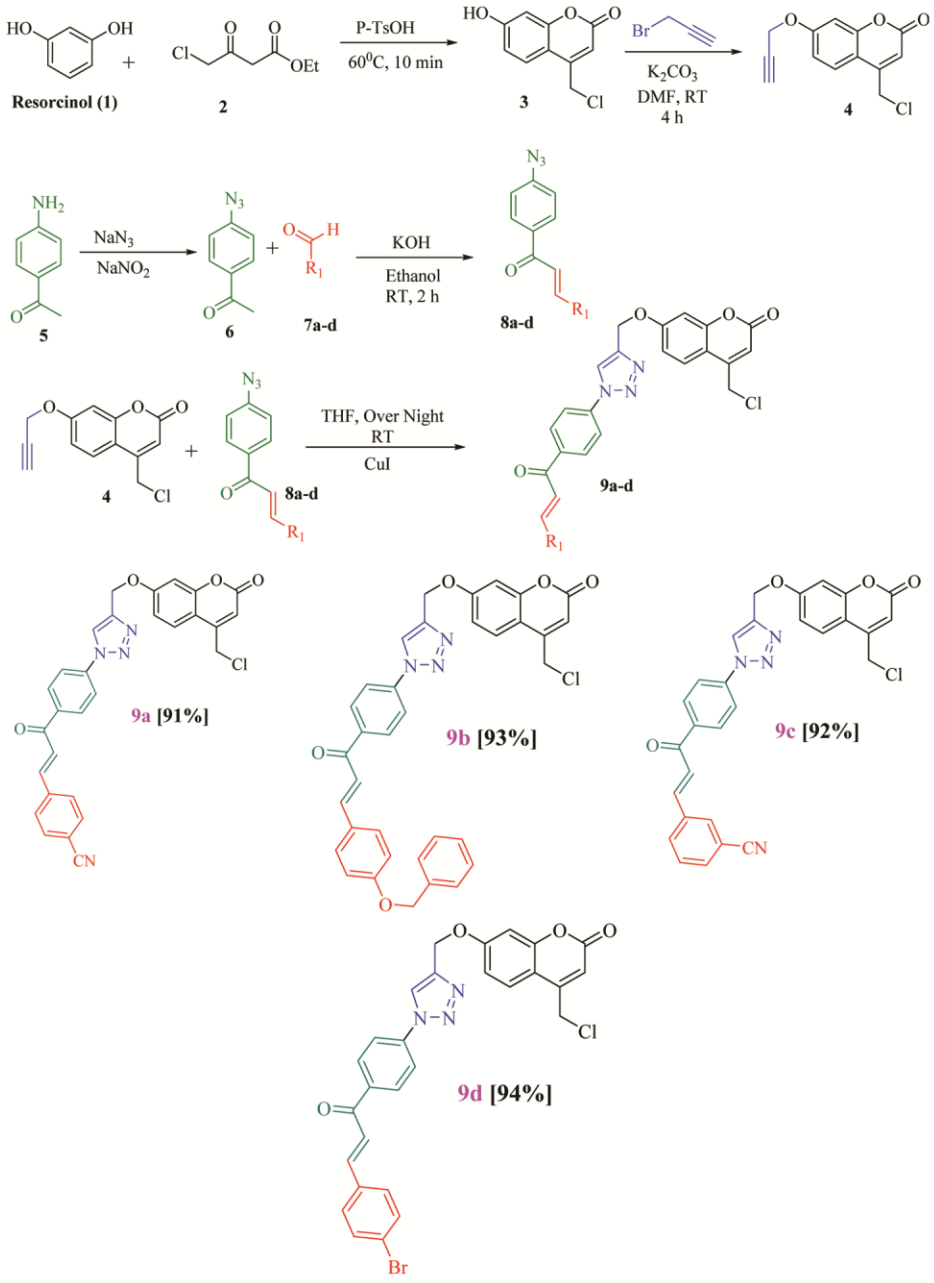

Scheme 1 — Synthesis of novel coumarin-1,2,3-triazole-chalcones

Also further confirmed by the mass spectral studies, **9a** molecular ion peak was obtained at 594.1 $(M+ H_2O)^+$. The synthetic yields, molecular weights, Mass and NMR spectra of all the compounds were described in the experimental section.

Antiproliferative activity

All the synthesized analogues were tested for their anticancer activity potentials in *in vitro* mode using MTT assay against selected human cancer cell lines such as A549 (lung cancer), HeLa (Cervix carcinoma), PANC1 (pancreatic cancer), HT1080 (Fibrosarcoma) and HEK293 (Human embryonic kidney cells). Majority of the compounds have exhibited moderate anticancer activity except compound **9a**, a *para*-nitrile chalcone, which has shown significant IC_{50} values in the range of 3.1 to 7.02 µg/mL (Table 1). All the synthesized derivatives have shown higher IC_{50} values against HEK 293 cell lines indicating their nontoxic nature towards normal cells.

Table 1 — Pharmacological activities of Coumarine-Triazole-chalcone derivatives **9a-d**

Compd	Anti -Cancer Activity (IC_{50} in µM/mL)				
	A549 (Lung Cancer)	HeLa (Cervix carcinoma cell line)	PANC-1 (Human Pancreatic Cancer Cell Line)	HT1080 (Human Fibrosarcoma cell line)	HEK293 (Human embryonic kidney cells)
9a	5.2 ± 0.17	6.2 ± 1.2	3.1± 0.8	7.02 ± 0.48	89.52 ± 9.2
9b	37 ± 1.2	23 ± 2.4	14 ± 0.564	35 ± 1.8	72.13 ± 8.5
9c	15 ± 1.2	43 ± 1.8	23 ± 1.36	39 ± 4.31	66.58 ± 3.8
9d	14.7±1.45	27.3 ± 4.13	19.1 ± 1.24	3.11 ± 0.97	88.11 ± 4.8
Doxo	0.8± 0.22	1.6 ± 0.42	3.8 ± 0.3	1.8 ± 0.4	64 ± 7.3

Table 2 — The binding interaction affinities of Ligands and inhibitors against SDH

Succinate Dehydrogenase (6VAX)				
Ligand	B.E. (Kcal/Mol)	Ki (µM)	Binding Pockets	H-Bond (Å)
9a	–11.2	6.081E-12	ARG451, ALA103, ALA102, HIS407, GLN104, GLU81, HIS407, TRP116, LEU306, TYR408, GLU440, HIS99, THR100, ALA441, GLY257, ALA72, GLY71, LEU460, GLY70, SER456, LEU457	LYS92 (3.45), LEU93 (3.47), GLU309 (3.55) GLU440 (3.98), THR308 (4.24)
9b	–11.7	2.613E-12	THR386, THR308, GLU81, TRP116, GLN104, GLY105, HIS407, ARG451, ALA103, THR271, SER272, GLY258, THR100, ALA69, THR91, GLY70, GLY68, ALA255, SER98, LEU460, GLU440, SER456, HIS99, GLY257, LEU457, LEU306, ALA102	THR100 (3.18) GLY70 (3.51) ALA69 (3.80) HIS99 (4.10) GLN104 (4.19)
9c	–10	4.616E-11	ARG451, SER98, GLY70, ALA69, LEU93, GLY257, GLY68, THR256, ALA255, GLU440, HIS99, THR100, TYR408, LEU460, GLY106, ALA103, HIS407, ALA454, GLY105, SER456	ALA193 (4.74) HIS99 (4.98)
9d	–11.2	6.081E-12	ALA454, GLY105, GLY106, LEU457, ARG451, THR100, TYR408, GLY70, GLY73, ALA72, ALA69, GLY71, THR256, ALA255, SER98, GLY257, GLY258, SER272, THR271, LEU460, GLU440, HIS99, SER456, ALA103, TRP116, THR267, LEU80, GLU81, GLN104, LEU306, HIS407, ALA102	GLY70 (3.61)(3.62) THR271 (4.35) ALA255(4.44)
Malonate	–5.0	0.000214851	GLU564, ASP15, THR50, ASP51, SER509, ARG507, PHE552, GLU159, ARG512, LEU158	SER509 (3.57) LEU158 (3.62)(4.17) THR508 (3.92)

In silico molecular docking

In silico docking studies of ligands with succinate dehydrogenase

In silico approaches provide a basis for assessing the efficacy of compounds against molecular targets, contributing to the selection of those that exhibit significant potential activity for further *in vitro* and *in vivo* study. In this study, synthesised compounds were docked with the key metabolic enzymes succinate dehydrogenase, which is accountable for cell viability[26]. Compounds showed substantial binding affinity compared to its known inhibitor. The Binding energy and pocket for each ligand with SDH protein are summarised in Table 2. Then, we further validated the *in-silico* findings by performing MTT assay. In the MTT assay, compound **9a** showed the highest IC_{50} at 3 to 7 µM on tested cancer cells. Based on cytotoxicity results, **9a** was selected for further target prediction study.

AKT as a potential target of 9a

PI3K/AKT has been identified as the intracellular protein that undergoes the most frequent modulation and is consequently implicated in a variety of human malignancies[27]. The proliferation, invasion, and metastasis of tumor cells are all facilitated by this route, which acts on various downstream target proteins. We searched the previous literature and found that PI3K and AKT are more common target biomarkers in Pancreatic cancer[28], Lung cancer[29], Cervical cancer[30] and Fibrosarcoma[31]. Hence, molecular docking was performed to analyze the binding capability of **9a** and different known inhibitors against the target proteins AKT and PI3K. In the results analysis (Table 3 and Table 4) **9a** showed a good binding

Table 3 — The binding interaction affinities of 9a and inhibitors against PI3K protein

			PI3K (8EXL)	
Ligands	B.E. (Kcal/Mol)	Ki (μM)	Binding Pockets	H-bond (Å)
9a	–10.3	2.78101E–08	ASP454, LEU452, GLY1007, ASN457, LYS640, PRO607, GLY363, ARG401, THR462, TYR641, VAL461, GLY460, PRO449, ILE459, GLN1014, PHE1016	GLN1014 (4.5)
Buparlisib	–8.7	4.14876E–07	LYS802, ASP933, ILE932, ILE848, TYR836, GLU849, PHE930, VAL851, MET922, ARG770, GLN859, ILE800, PRO778, MET772	ASP933 (4.3)
Pictilisib	–9.5	1.07414E–07	ARG818, GLU821, PRO835, ASN756, GLU849, HIS759, PHE794, ARG852, ASN797, ARG281, GLU798, ASN796	ASN797 (4)
Copanlisib	–8.1	1.14304E–06	ASP431, MET441, ASN428, GLN682, GLY463, THR462, LEU645, LYS640, THR679, VAL680, ARG683, VAL461, SER464, LYS468, GLU135, ILE427, ASP133	ASN428 (3.6) ARG683 (3.9)
Pilaralisib	–9.8	6.47126E–08	THR679, TYR641, GLN1014, TRP424, GLY1009, ASP454, ASN457, SER1015, PRO458, PHE1016, GLY460, LEU452, ILE459, VAL461, LEU1006, GLY1007, LYS640	ILE459 (4.7)
Sonolisib	–7.4	3.72875E–06	ARG281, LEU834, SER275, LYS924, ARG818, GLU849, HIS759, ASN756, ASN797, PHE794, ARG852, ASN796, GLU798, VAL850, LEU793	ARG852 (3.4)
Doxorubicin	–12.7	4.82645E–10	ARG852, ASN853, VAL850, MET922, GLU849, TYR836, ILE932, ILE848, ILE800, ARG770, THR856, MET772, GLN859, TRP780, SER854	SER854 (2.9) SER854 (4.1) VAL851 (3.4) VAL851 (2.9)

Table 4 — The binding interaction affinities of **9a** and inhibitors against AKT protein

			AKT (1O6L)		
Ligands	B.E. (Kcal/Mol)	Ki (μM)	Binding Pockets	Common Binding Residues	H-bond (Å)
9a	–10.6	1.67545E–08	LYS191, GLU193, LYS277, GLY161, ASP293, VAL166, THR292, TYR231, GLU230, ALA179, MET282, LEU158, ALA232, PHE439, GLY159, GLU236, LYS160, LYS181, PHE163	GLY161, GLY159, LYS160, LYS181, GLU236, PHE163, VAL166, LYS277, ASP293,	ALA232 (3.1)
Ipatasertib	–8.7	4.14876E–07	LYS160, GLU236, GLY159, GLY161, VAL166, GLY164, LYS181, PHE163, ASP293, LEU296, LEU183, GLU200, GLU193, GLY295, HIS196, THR197, THR162	LYS160, LYS181, GLU236, GLU200, GLU193, GLY159, GLY161, PHE163, VAL166	–
MK-2206	–9	2.49946E–07	LYS160, GLY159, VAL166, ASP293, LYS181, GLY164, GLU200, LEU183, THR197, HIS196, GLU193, THR162, PHE163, LYS277, GLY161, GLU236	LYS160, LYS181, LYS277, GLY159, GLY161, VAL166, ASP293, PHE163, GLU193, GLU236	GLU193 (3.6)
Capivasertib	–8.9	2.9594E–07	MET282, ASN280, GLU279, VAL166, PHE439, TYR231, ALA179, LYS181, MET229, ALA232, ASP293, THR292, GLY159, LEU158, LYS277, LYS160, GLU236, GLY161	MET282, GLU236, VAL166, PHE439, TYR231, ALA232, ASP293, GLY161, GLY159, LEU158, LYS277, LYS160	ASP293 (3.9)
Afuresertib	–8.7	4.14876E–07	GLY164, PHE163, GLY161, LYS160, GLY159, THR292, VAL166, ALA232, THR213, GLU230, ALA179, PHE439, LEU158, GLU236, LYS181, MET282, GLU279, LYS277, ASP293	GLY161, GLY159, PHE163, PHE439, LYS160, LYS181, LYS277, MET282, ASP293, ALA179, ALA232, GLU230, GLU236, VAL166	ALA232 (3.6)
Uprosertib	–8.8	3.50398E–07	GLU279, ASN280, PHE163, ASP293, LEU296, ASP275, GLY295, THR197, ILE188, GLU193, LEU183, LYS181, GLY164, GLY161, VAL166, GLY159, GLU236, LYS160	GLU236, GLU193, PHE163, ASP293, LYS160, LYS181, VAL166, GLY161, GLY159	GLU279 (4.2) ASP293 (4.2)
Doxorubicin	–12.3	9.48543E–10	ASP293, THR292, VAL166, LYS181, MET229, ALA179, ALA232, LEU158, GLY159, PHE439, MET282, GLU236, PHE443, LYS160	ASP293, THR292, VAL166, LYS181, ALA179, ALA232, LEU158, PHE439, MET282, GLU236, LYS160	ASP293 (4.9)

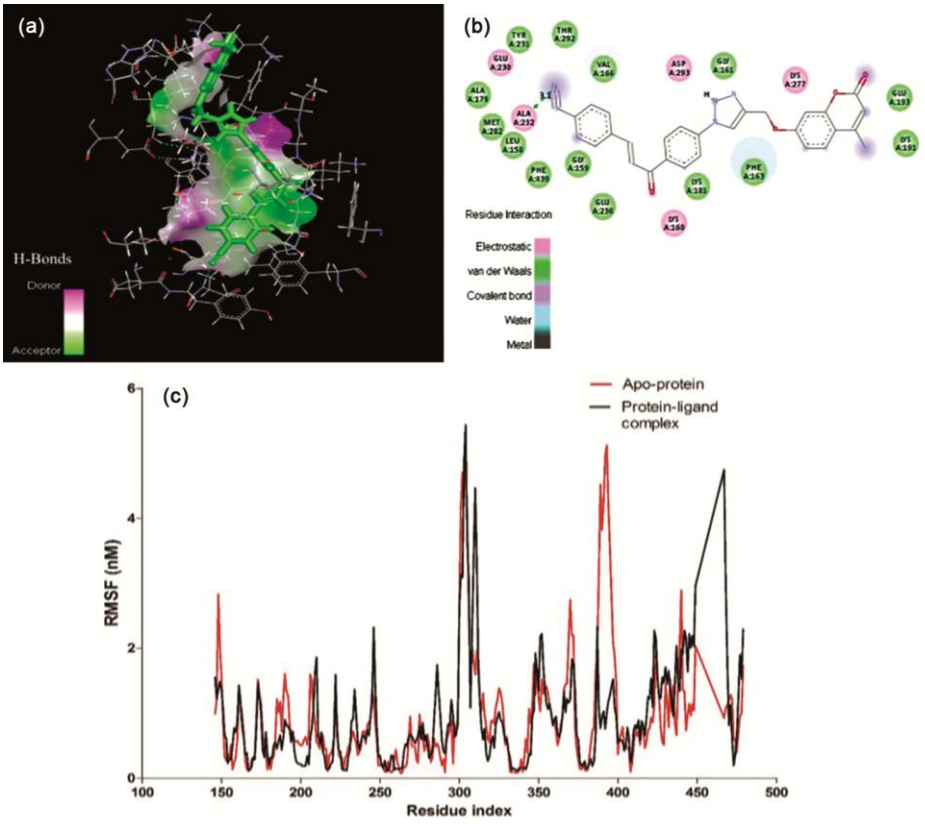

Fig. 2 — Binding interaction and simulation of **9a** with AKT protein in (A) 3D representation of binding pocket, (B) 2D representation of binding pocket, (C) Root mean square fluctuation plot of apo-protein and protein-ligand complex.

Table 5 — Drug likeness properties of compound **9a**

Compd	Molecular weight (g/mol)	Lipophilicity (M log P)	H-bond (Donors)	H-bond (Acceptors)	Molar refractivity
9a	522.95	5.20	0	8	144.51

affinity with AKT (-10.6) and PI3K (-10.3). However, upon observing the binding pockets of docked complex, it was found that the **9a**, doxorubicin, and AKT inhibitors such as ipatasertib, MK-2206, capivasertib, afuresertib, uprosertib possess similar amino acid residues (ASP293, THR292, VAL166, LYS181, ALA179, ALA232, LEU158, PHE439, MET282, GLU236, LYS160, GLY161, GLY159, PHE163, LYS277) in the binding pocket as compared to PI3K inhibitors. On this basis, AKT was screened out to be the most probable target and further subjected to simulation studies.

Simulation study deciphers the root mean fluctuations of receptor-ligand complexes. We plotted the RMSF values of apo-protein and protein-ligand complex to assess the influence of the drug on structural stability and integrity. The RMSF estimates how often atoms or groups of atoms move in respect to the related structure.

Drug likeness reveals that the compound is unsuitable for the oral administration route as it violates the Lipinski rule of five; however, it may have other administration routes, such as intravenous and intraperitoneal routes. The ADMET study affirms that **9a** has an excellent pharmacokinetic profile as it did not inhibit the CYP450 enzymes and is non-permeable to BBB and CNS. Additionally, it showed no carcinogenicity or skin toxicity. A better understanding of the interactions between **9a** and AKT protein is provided by molecular docking and dynamics studies which implicated that **9a** has high effectiveness as a druggable target for AKT protein as compared to its inhibitors (Fig. 2). The current findings provide substantial evidence that AKT protein is a potential target of **9a**, highlighting a novel aspect of its therapeutic value (Table 5 and Table 6).

Table 6 — *In silico* ADMET analysis of compound **9a**

Adsorption			Distribution			Metabolism	Excretion		Toxicity		
Caco2 Permeability	MDCK Permeability	Intestinal absorption	BBB Permeability	CNS Permeability	VD	CYP450 Inhibitor	CL	T1/2 (min)	AMES toxicity	hERG Blockers	Skin Sensitisation
–4.860	1e–05	100	–1.314	–2.172	0.490	No	6.085	0.137	No	No	No

Conclusion

In conclusion, a convenient and efficient method for the synthesis of novel hybrids of Coumarin with Chalcones linked with 1,4-disubstituted 1,2,3-triazoles by using 1,3-dipolarcycloadditon reaction and aldol condensations was developed. The predictable regiochemistry and stereochemistry of cycloaddition, and the generally high yields of cycloadducts, ensure that this will find a widespread application in the area of organic and medicinal chemistry. The MTT assay results shown that the 4-cyano chalcone derivative has significantly inhibited the selected human cancer cell lines in Fibrosarcoma cell line (HT1080). Further, **9a** was found to be more selective towards binding of AKT target out of tested PI3K/AKT targets during *in silico* docking studies, throwing more hopes towards its anticancer drug development possibilities.

Supplementary Information

Supplementary information is available in the website http://nopr.niscpr.res.in/handle/123456789/58776.

Acknowledgements

The authors thank the director, CSIR-CIMAP, Lucknow, for his constant encouragement and support. Author Akanksha Singh is thankful to Academy of Scientific and Innovative Research (AcSIR), Ghaziabad, Uttar Pradesh, India for providing financial assistance.

Disclosure statement

The Authors declare no competing financial interest.

References

1 Vladimir V K & Alicia G B, *Eur J Med Chem*, 44 (2009) 3091.
2 Sahoo S S, Shukla S, Nandy S & Sahoo H B, *Eur J Exp Biol*, 2 (2012) 899.
3 Olayinka AO & Obinna N C, *J Heterocycl Chem*, 47 (2010) 179.
4 Agalave S G, Maujan S R & Pore V S, *Chem Asian J*, 6 (2011) 2696.
5 Soltis M J, Yeh H J, Cole K A, Whittaker N, Wersto R P & Kohn E C, *Drug Metab Dispos*, 24 (1996) 799.
6 Reddy D M, Srinivas J, Chashoo G, Saxena A K & Kumar S H M, *Eur J Med Chem* 46 (2011) 1983.
7 Devendar P, Niranjana K A, Srinivas S K V N, Kumar K J, Singh S, Meena A, Misra P & Luqman S, *J Heterocycl Chem*, 58 (2021) 2090.
8 Yakaiah C, Manjulath K, Sharma P, Srinivas S K V N, Jonnala K, Kumar N A, Khan F & Setty O H, *J Heterocycl Chem*, 53 (2016) 1902.
9 Odlo K, Chabert F D J, Ducki S, Gani O A B S M, Sylte I & Hansen T V, *Bioorg Med Chem*, 18 (2010) 6874.
10 Lee S J, *Bull Korean Chem Soc*, 32 (2011) 737.
11 Pertino M W, Verdugo V, Theoduloz C & Hirschmann S G, *Molecules*, 19 (2014) 2523.
12 Cheng J H, Hung C F, Yang S C, Wang J P, Won S J & Lin C N, *Bioorg Med Chem*, 16 (2008) 7270.
13 Nielsen S F, Boesen T, Larsen M, Schonning K & Kromann H, *Bioorg Med Chem*, 12 (2004) 3047.
14 Zhan C & Yang J, *Pharmacol Res*, 53 (2006) 303.
15 Liu M, Wilairat P & Go M L, *J Med Chem*, 44 (2001) 4443.
16 Go M L, Wu X & Liu X, *Curr Med Chem*, 12 (2005) 481.
17 (a) Sabzevari O, Galati G, Moridani M Y, Siraki A & O'Brien P, *J Chem Biol Interact* 148 (2004) 57; (b) Lee Y S, Lim S S, Shin K H, Kim Y S, Ohuchi K & Jung S H, *Biol Pharm Bull*, 29 (2006) 1028; (c) Rozmer Z, Berki T & Perjesi P, *Toxicol In Vitro*, 20 (2006) 1354.
18 Komuraiah B, Kumar N A, Srinivas S K V N, Kumar K J, Chinde S, Kumar A D, Kumar Y, Grover P, Ashok T & Khan F, *J Heterocycl Chem*, 58 (2021) 2078.
19 Yakaiah C, Sneha T, Shalini T, Chinde S, Kumar A D, Kumar N A, Srinivas S K V N, Sarfaraz A, Kumar K J, Khan F, Ashok T & Grover P, *Eur J Med Chem*, 93 (2015) 564.
20 Edet L & Hemalatha M S, *Appl Biochem Biotech* (2022) 215. (https://doi.org/10.1007/s12010-021-03791-7).
21 Jha V, Bhosale A, Kapadia P, Bhargava A, Marick A, Charania Z & Madaye B, *J Appl Biol Biotech*, 11 (2023) 116.
22 Vardhan S & Sahoo S K, *Comp Biology Medicine*, 124 (2020) 103936.
23 Ismail S Y & Uzairu A, *Radiology Infec Diseases*, 6 (2019) 108.
24 Kharisma V D, Ansori A N M, Dian F A, Rizky W C, Dings T G A, Zainul R & Nugraha A P, *Biochem Cell Archives*, 21 (2021) 3323.
25 Dulsat J, López-Nieto B, Estrada-Tejedor R & Borrell J I, *Molecules*, 28 (2023) 776.
26 Ghasemi M, Turnbull T, Sebastian S & Kempson I, *Int J Mol Sci*, 22 (2021) 12827.
27 Rascio F, Spadaccino F, Rocchetti M T, Castellano G, Stallone G, Netti G S & Ranieri E, *Cancers* (*Basel*), 13 (2021) 3949.
28 Wang S, Zheng Y, Yang F, Zhu L, Zhu X Q, Wang Z F & Dong Q Z, *Sig Transduct Target Therap*, 6 (2021) 249.
29 Coates D R, Chin J M & Chung S T L, *Bone*, 23 (2011) 1.
30 Volkova L V, Pashov A I & Omelchuk N N, *Int J Mol Sci*, 22 (2021) 1.
31 Rijs Z, Shifai A N, Bosma S E, Kuppen P J K, Vahrmeijer A L, Keereweer S & Van Driel P B A A, *Cancers*, 13 (2021) 1